Zintl Phases

DOI: 10.1002/anie.200604356

$Na_{29}Zn_{24}Sn_{32}$: A Zintl Phase Containing a Novel Type of $\{Sn_{14}\}$ Enneahedra and Heteroatomic $\{Zn_8Sn_4\}$ Icosahedra**

*Sung-Jin Kim, Stephan D. Hoffman, and Thomas F. Fässler**

Homoatomic clusters are suitable candidates for the investigation of structure–property relationships at the borderline between molecules and solids. They can be functionalized, bridged, coupled, and polymerized in solution, and are therefore ideal building blocks for the design of tailored nanostructures.[1] In compounds of the electron-poor elements of Group 13, interesting parallels are found between the so-called metalloid clusters[2,3] (ligand-stabilized metal clusters that contain metal atoms not bonded to ligands, as well as noncovalent metal–metal interactions) and the interconnected clusters of intermetallic phases.[4] The cluster units of these intermetallic phases play a striking role in the three-dimensional array of atoms due to their notable stability. For instance, in metal borides, nonclassically bonded boron polyhedra are interconnected by covalent interactions.[5] In contrast, the polyhedra of typical closed-packed intermetallic phases, such as Frank–Kasper phases, are simply invoked to provide a better topological depiction of the structure.[4d]

Solid-state compounds of the elements of Group 13 often feature icosahedral building units, as demonstrated by α- and β-rhombohedral boron, metal borides, δ-gallium, and the extended cluster networks of alkali-metal indides and gallides.[4c] As counterparts in molecular chemistry, icosahedral $\{M_{12}\}$ units are found in soluble ligand-stabilized metal clusters such as $[Al_{77}R_{20}]^{2-}$,[6] $[Al_{22}Br_{20}(thf)_{12}]$,[7] and $[Ga_{12}R_{10}]^{2-}$.[8] Whereas such molecular metalloid clusters do not normally have closed-shell electronic configurations, electron-precise clusters that can be described by the rules of Zintl–Klemm–Busmann[9] and Wade[10] are common in the solid-state compounds mentioned above. Electron deficiencies in these structures can be compensated by the condensation of icosahedral units, for instance, through the sharing of faces.[11] In addition to numerous examples of homoatomic icosahedra, a few examples of heteroatomic icosahedra have been described, for instance, those found in $K_{34}Zn_{20}In_{85}$[12] and $Na_{102}Cu_{36}Ga_{279}$.[13] In some cases, the Group 13 elements (with three valence electrons) can be replaced by a combination of elements from Group 12 (with two valence electrons) and Group 14 (with four valence electrons), leading to an isoelectronic situation (with three valence electrons on average). Compounds such as $Mo_7Sn_{12}Zn_{40}$,[14a] $Na_{13}Cd_{20}E_7$ (E = Pb, Sn),[14b] and $Na_{49}Cd_{58.34}Sn_{37.69}$[14c] illustrate this principle.

It is noteworthy that no corresponding ternary alkali-metal compounds of zinc and tin have yet been described. Our research has focused on these systems, because in such compounds, structural motifs caused by electron deficiency are anticipated to compete with complex networks of covalently bonded tin atoms. Electron-deficient motifs are expected at balanced Sn/Zn ratios, in particular, whereas tin-rich phases should experience a transition known from the tin-rich side of the binary Na–Sn system, going with increasing tin content from Zintl phases with isolated tin clusters (Na_4Sn_4[15]), or two- or three-dimensional tin networks (Na_7Sn_{12},[16] $NaSn_2$,[17] and Na_5Sn_{13}[18]), to a phase with metallically bonded tin atoms ($NaSn_5$[19]).[20]

In $Na_{29}Zn_{24}Sn_{32}$, both building principles coexist: covalently linked $\{Zn_8Sn_4\}$ icosahedra coexist with a one-dimensional covalently bonded homoatomic tin substructure. The tin substructure contains a new type of polyhedron,[21] an enneahedron with 14 vertices, nine faces, and nearly equal edge lengths.

Single crystals with the composition $Na_{29}Zn_{24}Sn_{32}$ were obtained through the stoichiometric reaction of the elements in a tantalum ampoule at 450 °C.[22] The compound crystallizes in a new structure type in the primitive hexagonal space group $P\bar{6}_2m$ with the cell parameters $a = 15.712(1)$ and $c = 9.462(1)$ Å.[23a] The main structural features are linear chains of $\{Sn_{14}\}$ clusters, $\{Sn_3\}$ triangles, and $\{Zn_8Sn_4\}$ icosahedra.

A projection of the unit cell along the *c* axis (Figure 1a) illustrates the arrangement of these structural units in a three-dimensional network. The $\{Zn_8Sn_4\}$ icosahedra are assembled in a Kagomé net (Figure 1b) and are interconnected by four Sn–Zn contacts with $d(Sn2–Zn2) = 2.724(1)$ Å.[24] The atomic positions of the polyhedra are well-ordered, and the 30 edges consist of one Sn–Sn, 18 Sn–Zn, and 11 Zn–Zn contacts. The homoatomic intracluster contacts are longer than single bonds, whereas the intra- and intercluster Zn–Sn distances are of comparable lengths.[25] As outlined in Figure 1c, the $\{Zn_8Sn_4\}$ icosahedra of the nets perpendicular to the *c* axis are connected by the Zn2 atoms to the Sn1 atoms of the $\{Sn_3\}$ units between these layers with $d(Zn2–Sn1) = 2.829(1)$ Å. The $\{Sn_3\}$ units are located between the Kagomé layers, within the triangular channels of the Kagomé nets. Thus, together with a neighboring $\{Zn_3Sn_3\}$ hexagon and three additional zinc atoms, they form sodium-centered truncated tetrahedra, or Friauf polyhedra, if four additional sodium atoms capping the six-membered faces are considered (Figure 1d). The Friauf polyhedra are stacked along [001] by alternately

[*] S.-J. Kim, Dr. S. D. Hoffman, Prof. Dr. T. F. Fässler
Department Chemie
Technische Universität München
Lichtenbergstrasse 4, 85747 Garching (Germany)
Fax: (+49) 89-289-13186
E-mail: thomas.faessler@lrz.tum.de

[**] The authors thank Prof. M. Ruck, Prof. S. Alvarez, and Prof. S. Lidin for helpful discussions, and Dr. A. Schier for revising the manuscript.

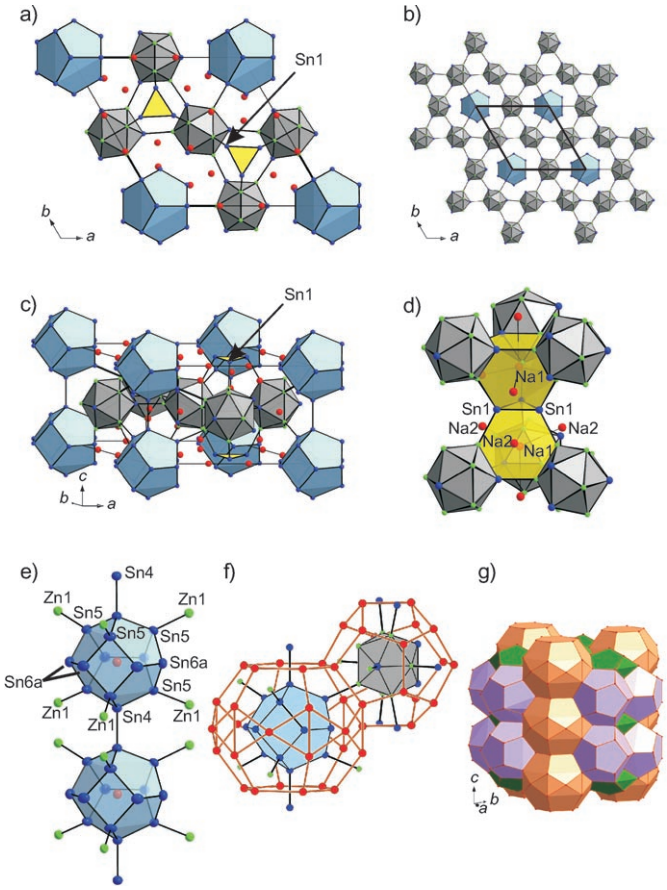

Figure 1. The structure of $Na_{29}Zn_{24}Sn_{32}$. a) The unit cell in projection along the *c* axis, highlighting the $\{Zn_8Sn_4\}$ icosahedra (gray), $\{Sn_{14}\}$ polyhedra (blue), and $\{Sn_3\}$ triangles (yellow); Na red, Zn green, Sn blue. b) The Kagomé net of $\{Zn_8Sn_4\}$ icosahedra parallel to the *ab* plane, as well as the embedded $\{Sn_{14}\}$ polyhedra (without the $\{Sn_3\}$ triangles and sodium atoms). c) The unit cell in projection perpendicular to the *c* axis, showing how the $\{Sn_3\}$ triangles bridge the $\{Zn_8Sn_4\}$ icosahedra. d) The interconnection of the truncated tetrahedra (yellow) and the $\{Zn_8Sn_4\}$ icosahedra along *c* direction. e) The linear chain of $\{Sn_{14}\}$ polyhedra along the *c* axis; displacement ellipsoids are set at 90% probability. f) A pair of interconnected $\{Sn_{14}\}$ and $\{Zn_8Sn_4\}$ clusters with the $\{Na_{30}\}$ and $\{Na_{20}\}$ cages surrounding them. g) The arrangement of the $\{Na_{20}\}$ (purple) and $\{Na_{30}\}$ (orange) cages, which results in voids (green).

sharing $\{Sn_3\}$ triangles and $\{Zn_3Sn_3\}$ hexagons and, thus, connect the layers of icosahedra (Figure 1 d).

A homoatomic tin substructure that can be described as a linear chain of $\{Sn_{14}\}$ polyhedra,[26] each of which encapsulates a sodium atom, is embedded in the larger hexagonal channels of the Kagomé framework (Figure 1 a,b). As shown in Figures 1 e and 4 (cluster **A**), the $\{Sn_{14}\}$ polyhedron consists of six pentagonal and three distorted square faces. The threefold principal rotation axis of the D_{3h}-symmetric polyhedron is identical to the crystallographic $\bar{6}$ rotation axis. The astoundingly simple polyhedron can be derived from a trigonal bipyramid by truncating the three equatorial vertices and compressing the bipyramid along the threefold axis. The faces are nearly planar and are only slightly distorted, with bond angles of 106.1–109.9° (sum 538.4°) for the pentagonal faces, and of 84–96° (sum 360°) for the square faces. The Sn–Sn distances are in the narrow region of $d(Sn{-}Sn) = 2.825(1)$–$2.993(1)$ Å and are in the range of distances of the covalent Sn–Sn interactions in α-tin. The enneahedra are covalently interconnected along the *c* axis by the atom shared by the three pentagonal faces (Sn4; $d(Sn4{-}Sn4) = 2.884(2)$ Å), generating a linear chain of clusters (Figure 1 e). Additionally, six other tin vertices (Sn5) of the polyhedron establish *exo*-cluster bonds to the Zn1 atoms of six surrounding $\{Zn_8Sn_4\}$ icosahedra ($d(Sn5{-}Zn1) = 2.914(1)$ Å). Twelve $\{Zn_8Sn_4\}$ icosahedra are positioned in a hexagonal prism surrounding the $\{Sn_{14}\}$ unit (Figure 2 a).

The sodium atoms coordinating the two cluster types form two different sodium polyhedra around the clusters (Figure 1 f): 20 sodium atoms capping the triangular faces of the icosahedra form a pentagonal dodecahedron, the dual polyhedron of the icosahedron; 30 sodium atoms encapsulating the $\{Sn_{14}\}$ cluster form an icosihexahedron with two hexagonal, 12 pentagonal, and 12 triangular faces.[27] The $\{Na_{30}\}$ polyhedra are fused by sharing hexagonal faces along the *c* axis; they also share pentagonal faces with neighboring $\{Na_{20}\}$ pentagonal dodecahedra (Figure 1 f,g). In contrast to the structure of clathrate I,[28] complete space-filling is not achieved with the $\{Na_{20}\}$ and $\{Na_{30}\}$ polyhedra, but the sodium polyhedra separate the structure into distinct homo- and heteroatomic substructures.

On the basis of the number of interatomic contacts, the electron count for $Na_{29}Zn_{24}Sn_{32}$ can be rationalized as follows: The 14 tin atoms of each enneahedron are covalently bonded to each other. In addition, six of them (Sn5) establish Sn–Zn *exo*-cluster contacts, and two (Sn4) establish Sn–Sn *exo*-cluster contacts. The assumption of completed valence shells leads to the formulation of $\{(4b\text{-}Sn)_8(3b\text{-}Sn)_6\}^{6-}$ (3b = three-bonded, 4b = four-bonded) for the enneahedron, where the three-bonded tin atoms have lone electron pairs. The $\{Zn_8Sn_4\}$ icosahedron can be regarded as analogous to the 26-skeletal-electron cluster *closo*-$B_{12}H_{12}^{2-}$. An *exo*-bonded Zn_{exo} atom contributes one electron, an *exo*-bonded Sn_{exo} atom three electrons, and a tin atom that is not *exo*-bonded two electrons to the cluster skeleton. Thus, the 10-fold *exo*-bonded $\{(Zn_{exo})_8(Sn_{exo})_2(Sn)_2\}$ icosahedron is assigned $8\times1+2\times3+2\times2=18$ skeletal electrons. A formal charge of −8 is needed to reach the 26 skeletal electrons required for a *closo* icosahedral cluster (that is, $2n+2$, where $n=12$). Assuming that the slightly long Sn–Sn contacts ($d(Sn1{-}Sn1) = 3.018(1)$ Å) of the $\{Sn_3\}$ unit are covalent interactions, all the tin atoms of this unit are four-bonded, resulting in a formal charge of 0.[29] For one $\{Sn_{14}\}^{6-}$, three $\{Zn_8Sn_4\}^{8-}$, and two $\{Sn_3\}^0$ units per unit cell, 30 sodium atoms are required to transfer their valence electrons to the sublattices, according to the Zintl–Klemm–Busmann concept.

The electron count was confirmed by extended Hückel calculations.[30] In Figure 3 a, the density of states (DOS) of the Sn–Zn sublattice is shown. When the states are filled successively with electrons (rigid band filling), the Fermi level (E_F) corresponding to $\{Zn_{24}Sn_{32}\}^{30-}$ lies in an energy gap of 1 eV. The Fermi level corresponding to $\{Zn_{24}Sn_{32}\}^{29-}$ lies at approximately 7.0 eV and cuts through a region of high DOS. As outlined by the projected DOS, this region consists mainly of states associated with the three-bonded Sn6 atoms of the

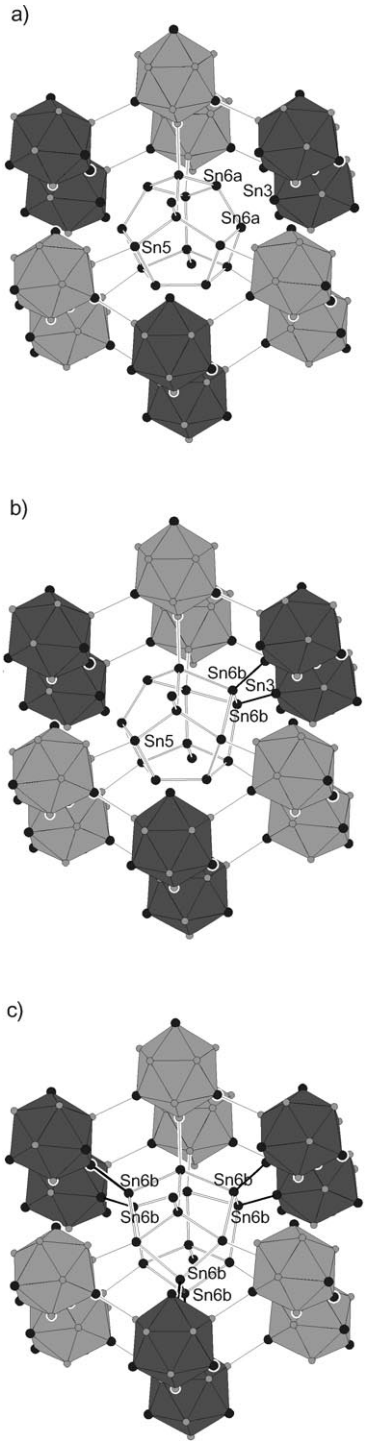

Figure 2. Isomers of the $\{Sn_{14}\}$ cluster and their interconnection with neighboring $\{Zn_8Sn_4\}$ icosahedra. a) The major $\{Sn_{14}\}$ isomer, in which the Sn6a sites are occupied; the $\{Sn_{14}\}$ cluster is connected by the Sn5 atoms to six $\{Zn_8Sn_4\}$ icosahedra; Zn small gray spheres, Sn large blackspheres. b) An $\{Sn_{14}\}$ isomer in which one pair of Sn6a atoms is replaced by a pair of Sn6b atoms, which establish two additional bonds to Sn3 atoms of $\{Zn_8Sn_4\}$ icosahedra. c) The $\{Sn_{14}\}$ isomer in which the Sn6b sites are occupied; the $\{Sn_{14}\}$ cluster is connected by the Sn5 and Sn6b atoms to 12 $\{Zn_8Sn_4\}$ icosahedra.

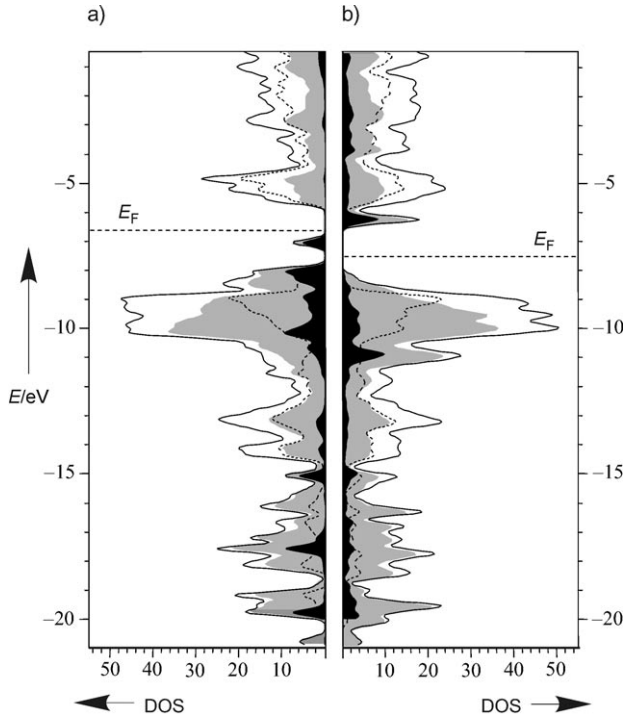

Figure 3. DOS of $Zn_{24}Sn_{32}$ models containing the two limiting isomers of the $\{Sn_{14}\}$ cluster. a) Model containing $\{Sn_{14}\}$ clusters in which the Sn6a sites are occupied (Figure 2a); the Fermi energy (E_F) for the $\{Zn_{24}Sn_{32}\}^{30-}$ substructure is indicated; total DOS: ——, Zn states: -----, Sn states: gray area, Sn6 states: black area. b) Model containing $\{Sn_{14}\}$ clusters in which the Sn6b sites are occupied (Figure 2c); the E_F for the $\{Zn_{24}Sn_{32}\}^{26-}$ substructure is indicated.

enneahedron (Figure 3a). The presence of an energetically separated region in the DOS near the Fermi level resembles the situation found for K_6Sn_{25} and $K_6Bi_2Sn_{23}$.[31] In these cases, the energy of the sp^3-hybridized orbitals of three-bonded tin atoms is raised by interactions among the lone electron pairs.[32]

The refinement of the crystallographic data led to a split model for the Sn6 position; in this model, the occupancy of the original Sn6a site is 92%, and that of the new Sn6b site is 8%.[23a] The effect of this disorder on the structure of the $\{Sn_{14}\}$ cluster is shown in Figure 4. Cluster **A**, which corresponds to the major disorder component, has three Sn6a–Sn6a contacts oriented parallel to the *ab* plane. This cluster is overlaid with a cluster in which one pair of Sn6b atoms

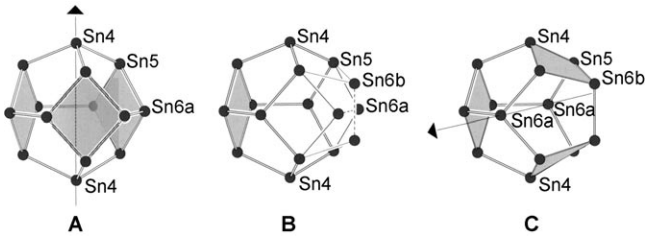

Figure 4. Disorder of the $\{Sn_{14}\}$ cluster. Cluster **A** corresponds to the major disorder component, in which the Sn6a sites are occupied. The rotation of one Sn6a–Sn6a unit (model **B**) leads to cluster **C**, in which one pair of Sn6b sites is occupied. Clusters **A** and **C** have the same number and types of vertices and faces, but the location of the (quasi-)threefold axis (arrow) has changed. See text for details.

replaces a pair of Sn6a atoms, in model **B**. The disorder corresponds to a rotation of a Sn6a–Sn6a unit in cluster **A** around an axis perpendicular to the bond vector. The outcome of this rotation is cluster **C**, which has the same number and types of vertices and faces as the initial cluster **A**. In cluster **C**, six interconnected pentagonal faces and three distorted square faces again generate an enneahedron; the now quasi-threefold rotation axis runs through opposite Sn6a atoms. As the simple rotation of one of the three Sn6–Sn6 units results in a topologically identical cluster, the process can be interpreted as a pseudorotation. However, cluster **C** is more distorted than cluster **A** and also has longer Sn6–Sn5 distances (d(Sn6–Sn5) = 3.208(6) Å). Through the pseudorotation, additional intercluster Sn–Sn contacts can be established (Figure 2b,c). The initially three-bonded Sn6 atoms are now able to form covalent bonds to tin atoms (which also formerly possessed an lone electron pair) of an adjacent icosahedron (d(Sn6b–Sn3) = 2.918(9) Å); consequently, all the vertices of the icosahedron have *exo*-cluster bonds.

Assuming that Sn6b sites are randomly occupied only once per cluster, $3 \times 8\% = 24\%$ of the polyhedra adopt shape **C**. With the formation of two extra bonds, the required electron count of the substructure is reduced to such an extent that an electron-precise Zintl phase results. For the isomeric structure that contains cluster **C**, the electron count is the following. The enneahedron is now counted as $\{(4b\text{-}Sn)_{10}(3b\text{-}Sn)_4\}^{4-}$. The $\{(Sn_{exo})_4(Zn_{exo})_8\}$ icosahedron is assigned $8 \times 1 + 4 \times 3 = 20$ skeletal electrons, and six additional electrons are required for an electron-precise Wade cluster. Thus, a total of 26 sodium atoms must donate their valence electrons to achieve one $\{Sn_{14}\}^{4-}$, one $\{Zn_8Sn_4\}^{6-}$, two $\{Zn_8Sn_4\}^{8-}$, and two $\{Sn_3\}^0$ units per unit cell. Weighting the structure as 76% of cluster **A** and 24% of cluster **C** leads to an average electron demand of $0.76 \times 30 + 0.24 \times 26 = 29.04$ electrons. This result is in good agreement with the 29 sodium atoms in the crystallographically determined chemical formula.

The lowering of the Fermi level by the creation of the additional bonds was confirmed by extended Hückel calculations[30] on a model containing exclusively Sn6b sites (Figure 2c). Owing to symmetry considerations, a model containing both cluster orientations could only be calculated using a very large unit cell and was, thus, beyond our computational capabilities. As expected, the band gap of approximately 2 eV in the DOS in Figure 3b is larger than that in Figure 3a, and the states contributed by the lone electron pairs, which lie near the Fermi level in Figure 3a, have vanished. This result is consistent with the assumption that no lone electron pairs are present in the structure containing the bonding scenario shown in Figure 2c. In $Na_{29}Zn_{24}Sn_{32}$, which contains statistically occupied split positions, the number of three-bonded Sn6 atoms is reduced precisely to the extent that the Fermi level lies above the states corresponding to the lone electron pairs of the three-bonded atoms.

The intermetallic compound presented herein demonstrates that the icosahedral building principle typical of the elements of Group 13 can also be extended to combinations of electron-richer and electron-poorer elements. Icosahedral clusters of such combinations of elements prove to be stable entities,[13,14,33] which in $Na_{29}Zn_{24}Sn_{32}$ allow both the formation of a substructure based on $\{Sn_{14}\}$ clusters and the isomerization of the $\{Sn_{14}\}$ clusters through pseudorotation. This isomerization provides a neat method for $Na_{29}Zn_{24}Sn_{32}$ to adjust its electron count to generate an electron-precise Zintl phase.

Received: October 24, 2006
Published online: March 13, 2007

Keywords: cluster compounds · polyhedra · tin · zinc · Zintl anions

[1] *Metal Clusters in Chemistry* (Eds.: P. Braunstein, L. A. Oro, P. R. Raithby), Wiley-VCH, Weinheim, **1999**; *Clusters and Colloids: From Theory to Applications* (Ed.: G. Schmid), VCH, Weinheim, **1994**.
[2] a) A. Schnepf, H. Schnöckel, *Angew. Chem.* **2002**, *114*, 3682; *Angew. Chem. Int. Ed.* **2002**, *41*, 3532; b) *Molecular Clusters of the Main Group Elements* (Eds.: M. Driess, H. Nöth), Wiley-VCH, Weinheim, **2004**.
[3] M. Brynda, R. Herber, P. B. Hitchcock, M. F. Lappert, I. Nowik, P. P. Power, A. V. Protchenko, A. Ruzicka, J. Steiner, *Angew. Chem.* **2006**, *118*, 4325; *Angew. Chem. Int. Ed.* **2006**, *45*, 4333.
[4] a) J. D. Corbett, *Angew. Chem.* **2000**, *112*, 682; *Angew. Chem. Int. Ed.* **2000**, *39*, 670; b) J. D. Corbett, *Struct. Bonding (Berlin)* **1997**, *87*, 158; c) M. Tillard-Charbonnel, C. Belin, *Prog. Solid State Chem.* **1993**, *22*, 59; d) T. F. Fässler, S. D. Hoffmann, *Angew. Chem.* **2004**, *116*, 6400; *Angew. Chem. Int. Ed.* **2004**, *43*, 6242.
[5] G. Schmid, *Angew. Chem.* **1970**, *82*, 920; *Angew. Chem. Int. Ed. Engl.* **1970**, *9*, 819.
[6] A. Ecker, E. Weckert, H. Schnöckel, *Nature* **1997**, *387*, 379.
[7] C. Klemp, R. Köppe, E. Weckert, H. Schnöckel, *Angew. Chem.* **1999**, *111*, 1851; *Angew. Chem. Int. Ed.* **1999**, *38*, 1739.
[8] J. Steiner, G. Stösser, H. Schnöckel, *Z. Anorg. Allg. Chem.* **2004**, *630*, 1879.
[9] a) E. Zintl, *Angew. Chem.* **1939**, *52*, 1; b) W. Klemm, *Proc. Chem. Soc. London* **1959**, 329; c) E. Busmann, *Z. Anorg. Allg. Chem.* **1961**, *313*, 90.
[10] K. Wade, *Adv. Inorg. Chem. Radiochem.* **1976**, *18*, 1.
[11] a) Examples of compounds with condensed icosahedra: $Na_{6.25}Rb_{0.6}Ga_{20.02}$,[11b] $Li_3Na_5Ga_{19.57}$,[11c] and $Na_{13}K_4Ga_{49.57}$;[11d] b) M. Charbonnel, C. Belin, *J. Solid State Chem.* **1987**, *67*, 210; c) M. Charbonnel, C. Belin, *Nouv. J. Chim.* **1984**, *10*, 595; d) C. Belin, M. Charbonnel, *J. Solid State Chem.* **1986**, *64*, 57.
[12] G. Cordier, V. Müller, *Z. Naturforsch. B* **1995**, *50*, 23.
[13] a) M. Tillard-Charbonnel, N. Chouaibi, C. Belin, J. Lapasset, *J. Solid State Chem.* **1992**, *100*, 220; b) M. Tillard-Charbonnel, C. Belin, *Prog. Solid State Chem.* **1993**, *22*, 59.
[14] a) V. Kuntze, K. Gebhardt, H. Hillebrecht, *Z. Kristallogr.* **1997**, *212*, 840; b) E. Todorov, S. C. Sevov, *Inorg. Chem.* **1997**, *36*, 4298; c) E. Todorov, S. C. Sevov, *J. Am. Chem. Soc.* **1997**, *119*, 2869.
[15] W. Müller, K. Volk, *Z. Naturforsch. B* **1977**, *32*, 709.
[16] T. F. Fässler, S. Hoffmann, *Inorg. Chem.* **2003**, *42*, 5474.
[17] F. Dubois, M. Schreyer, T. F. Fässler, *Inorg. Chem.* **2005**, *44*, 477.
[18] J. T. Vaughey, J. D. Corbett, *Inorg. Chem.* **1997**, *36*, 4316.
[19] C. Kronseder, T. F. Fässler, *Angew. Chem.* **1998**, *110*, 1641; *Angew. Chem. Int. Ed.* **1998**, *37*, 1571.
[20] T. F. Fässler, *Z. Anorg. Allg. Chem.* **2006**, *632*, 1125.
[21] The polyhedron is not a member of the 92 Johnson polyhedra; S. Alvarez, *Dalton Trans.* **2005**, 2209.
[22] For the synthesis of $Na_{29}Zn_{24}Sn_{32}$, stoichiometric amounts of the elements sodium, tin, and freshly distilled zinc were loaded into a tantalum ampoule under an inert gas. After sealing the

ampoule, the sample was heated to 450 °C at a rate of 2 K min^{-1} and then slowly cooled to room temperature at a rate of 0.1 K min^{-1}. The product contained the air-sensitive target compound as a crystalline powder with metallic luster. The powder X-ray diffractogram indicated the presence of small amounts of β-NaSn and another unknown phase.

[23] a) A single crystal of $Na_{29}Zn_{24}Sn_{32}$ was sealed in a glass capillary (0.3-mm diameter, Hilgenberg) in an argon-filled glove box. Crystal data: $0.15 \times 0.05 \times 0.05$ mm^3, $a = 15.712(1)$, $c = 9.462(1)$ Å, $V = 2022.9(2)$ Å^3, space group $P\bar{6}_2m$ (no. 189), $Z = 1$, $\rho_{calcd} = 4.953$ g cm^{-3}, $\mu(Mo_{K\alpha}) = 16.78$ mm^{-1}. Data collection: Oxford Diffraction Xcalibur3 diffractometer, 293(2) K, $Mo_{K\alpha}$ radiation, $2\theta_{max} = 55.58°$, 15973 reflections measured, 1801 independent reflections, $R_{int} = 0.039$, $R_1 = 0.024$ ($I \geq 2\sigma(I)$), $wR_2 = 0.059$ ($I \geq 2\sigma(I)$), $R_1 = 0.027$ (all data), $wR_2 = 0.058$ (all data). The crystal structure was solved using direct methods (SHELXS-97[23b]) and refined on F^2 by full-matrix least-squares methods (SHELXL-97[23c]), with anisotropic displacement parameters for all atoms. Of all the possible space groups that fulfilled the systematic extinction conditions, only $P\bar{6}_2m$ produced a successful model. No further symmetry elements were found (PLATON/ADDSYM[23d]). The Flack parameter[23e] of 0.01(3) indicates that the absolute structure is correct (a value of 0.5 would be expected for a racemic twin or if a center of inversion were present). Despite a well-converged refinement ($R_1 = 0.027$ (all data)), a residual electron-density peak (ca. 4.5 e Å^{-3}) remained near the three-bonded Sn6 site. Furthermore, the anisotropic displacement parameters of Sn6 ($U_{iso} = 0.0281(2)$ Å^2) were slightly bigger than those of the other tin positions. Therefore, a split model was introduced for the Sn6 site. Attempts to refine the residual electron-density peak as a partially occupied sodium or oxygen site did not result in a satisfying model, for geometric and electronic reasons. In the split model, the occupancy of the original Sn6a site refined to 92.4(2) %; in the final refinement, the occupancy of Sn6a was fixed at 92 % and that of the new Sn6b site at 8 %. The isotropic displacement parameter of the sites refined to $U_{iso} = 0.0238(2)$ Å^2. There was no indication for the presence of a superstructure. Further details on the crystal structure investigations may be obtained from the Fachinformationszentrum Karlsruhe, 76344 Eggenstein-Leopoldshafen, Germany (fax: (+49) 7247-808-666; e-mail: crysdata@fiz-karlsruhe.de), on quoting the depository number CSD-417144; b) G. M. Sheldrick, SHELXS-97, Program for the Solution of Crystal Structures, Universität Göttingen (Germany), **1997**; c) G. Sheldrick, SHELXL-97, Program for the Refinement of Crystal Structures, Universität Göttingen (Germany), **1997**; d) A. L. Spek, PLATON, A Multipurpose Crystallographic Tool, Utrecht University (The Netherlands), **2006**; e) H. D. Flack, *Acta Crystallogr. Sect. A* **1983**, *39*, 876.

[24] A similar arrangement of icosahedra is found in $Na_8K_{23}Cd_{12}In_{48}$.[33] In this structure, $\{In_{12}\}$ icosahedra are linked by $\{In_3\}$ units, resulting in a three-dimensional network. In contrast to the covalently bonded tin substructure of $Na_{29}Zn_{24}Sn_{32}$, the channels of the framework of icosahedra are filled with $\{Cd_{12}In_6\}$ double hexagonal antiprisms in $Na_8K_{23}Cd_{12}In_{48}$ and those determine the metallic nature of the compound.

[25] a) The average Zn–Zn distance and the Sn–Sn distance in the $\{Zn_8Sn_4\}$ cluster are $d(Zn–Zn)_{\varnothing} = 2.759$ Å and $d(Sn–Sn) = 3.038(1)$ Å. For comparison, the interatomic distance in elemental zinc is $d(Zn–Zn) = 2.665$ Å, and the average interatomic distance in the $\{Sn_{14}\}$ substructure is $d(Sn–Sn)_{\varnothing} = 2.909$ Å. The intracluster Zn–Sn distances are $d(Zn–Sn) = 2.729(2)$–$2.856(1)$ Å, and the corresponding *exo*-cluster contacts are $d(Zn–Sn) = 2.724(1)$–$2.914(1)$ Å. b) $Mo_7Sn_{12}Zn_{40}$[14a] contains molybdenum-centered icosahedra of composition $\{MoZn_{10}Sn_2\}$ with Zn–Sn distances similar to those in $Na_{29}Zn_{24}Sn_{32}$.

[26] a) A part of the complex network structure of the intermetallic phase Ag_7Te_4[26b] can be interpreted as a highly elongated variant the $\{Sn_{14}\}$ polyhedron; b) R. M. Imamov, Z. G. Pinsker, *Kristallografiya* **1966**, *11*, 182.

[27] A similar cage is found in the tetrakaidecahedron, a 24-vertex polyhedron with two hexagonal and 12 pentagonal faces. Tetrakaidecahedra occur together with pentagonal dodecahedra in the clathrate-I structures of $[(H_2O)_{46}Br_8]$[28a] and K_8E_{46-x} (E = Si, Ge, Sn).[28b] In the tetrakaidecahedron, the hexagonal faces are staggered, whereas in the present icosihexahedron they are eclipsed.

[28] a) M. von Stackelberg, H. R. Müller, *J. Chem. Phys.* **1951**, *19*, 1319; b) J. Gallmeier, H. Schäfer, A. Weiss, *Z. Naturforsch. B* **1969**, *24*, 665.

[29] a) $\{Sn_3\}$ units with a formal charge of −3 and comparable Sn–Sn distances ($d(Sn–Sn) = 3.059$ Å) occur in $BaSn_3$. Band-structure calculations demonstrated the covalent nature of the Sn–Sn bond;[29b] b) C. Kronseder, T. F. Fässler, *Angew. Chem.* **1997**, *109*, 2800; *Angew. Chem. Int. Ed. Engl.* **1997**, *36*, 2683.

[30] Extended Hückel calculations were carried out by using the MEHMACC software package; U. Häußermann, S. Wengert, R. Nesper, T. F. Fässler, MEHMACC, Program based on the QCPE Extended Hückel Program EHMACC, Zürich (Switzerland), **1993**.

[31] T. F. Fässler, *Z. Anorg. Allg. Chem.* **1998**, *624*, 569.

[32] In $Na_{29}Zn_{24}Sn_{32}$, the distances between the three-bonded Sn6 atoms of the $\{Sn_{14}\}$ unit and the Sn3 atoms of the $\{Zn_8Sn_4\}$ icosahedron are comparable to the distances between three-bonded tin atoms in K_6Sn_{25}.[31]

[33] D. M. Flot, M. Tillard-Charbonnel, C. Belin, *J. Am. Chem. Soc.* **1996**, *118*, 5229.

